Bio-Design and Manufacturing (2024) 7:889–898
https://doi.org/10.1007/s42242-024-00296-0

RESEARCH ARTICLE

Hierarchical structures on platinum–iridium substrates enhancing conducting polymer adhesion

Linze Li[1] · Changqing Jiang[2] · Luming Li[2,3]

Received: 29 September 2023 / Accepted: 26 May 2024 / Published online: 26 July 2024

Abstract

Conducting polymers (CPs), including poly(3,4-ethylenedioxythiophene):poly(styrenesulfonate) (PEDOT:PSS), are promising coating materials for neural electrodes. However, the weak adhesion of CP coatings to substrates such as platinum–iridium is a significant challenge that limits their practical application. To address this issue, we used femtosecond laser-prepared hierarchical structures on platinum–iridium (Pt–Ir) substrates to enhance the adhesion of PEDOT:PSS coatings. Next, we used cyclic voltammetry (CV) stress and accelerated aging tests to evaluate the stability of both drop cast and electrodeposited PEDOT:PSS coatings on Pt–Ir substrates, both with and without hierarchical structures. Our results showed that after 2000 CV cycles or five weeks of aging at 60 °C, the morphology and electrochemical properties of the coatings on the Pt–Ir substrates with hierarchical structures remained relatively stable. In contrast, we found that smooth Pt–Ir substrate surfaces caused delamination of the PEDOT:PSS coating and exhibited both decreased charge storage capacity and increased impedance. Overall, enhancing the stability of PEDOT:PSS coatings used on common platinum–iridium neural electrodes offers great potential for improving their electrochemical performance and developing new functionalities.

Graphic abstract

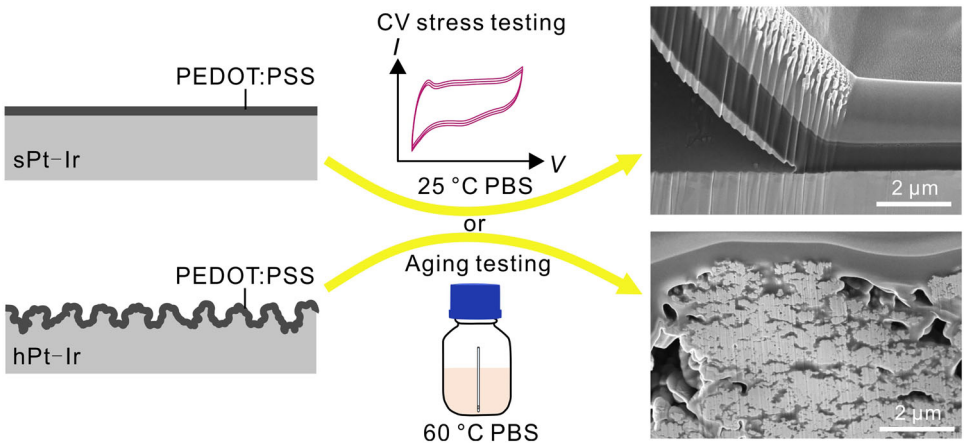

Keywords Hierarchical structures · Femtosecond laser · Conducting polymers · Neural electrodes · Stability

✉ Linze Li
lzli@fzu.edu.cn

✉ Changqing Jiang
jiangcq13@tsinghua.edu.cn

[1] School of Mechanical Engineering and Automation, Fuzhou University, Fuzhou 350108, China

[2] National Engineering Research Center of Neuromodulation, School of Aerospace Engineering, Tsinghua University, Beijing 100084, China

[3] IDG/McGovern Institute for Brain Research at Tsinghua University, Beijing 100084, China

Introduction

Implanted electrodes are essential components for neuromodulation devices and brain–computer interfaces [1]. For these applications to offer safe neural stimulation and effective recording, the electrode interface must permit sufficient charge injection with a stable and low impedance [2]. Conducting polymers (CPs) offer excellent electrochemical performance, biocompatibility, and versatility, which make them a popular coating for bioelectronic devices [3]. CP coatings have been found to be useful not only for neurobiochemical detection [4, 5] and closed-loop neuromodulation [6], but are also ideal coatings for ultralow frequency [7] or direct current stimulation [8–10] because of their high charge injection capacity [11]. In addition, they have been considered as potential drug delivery system candidates [12].

Although many CPs have been identified, poly(3,4-ethylenedioxythiophene):poly(styrenesulfonate) (PEDOT:PSS) is the prototypical CP used to coat neural electrodes [13, 14]. However, the lack of stable adhesion between PEDOT:PSS coatings and metal surfaces such as platinum or gold poses risks of delamination and shedding [15]. This can interrupt clinical treatment [16] and cause tissue damage [17], thereby endangering patient safety.

Various attempts have been made to address the weak adhesion of CP coatings. These efforts can be divided into two main categories: chemical and physical methods [14, 18]. Chemical methods involve the modification of the substrate material itself via chemical modification to enhance the stability of the coating. Examples of chemical methods include the use of 3,4-ethylenedioxythiophene (EDOT) acid [19], electrografting an amine-functionalized EDOT derivative [16], adding a hydrophilic polyurethane adhesive coating [20], and electrodeposition of poly(5-nitroindole) conductive films [21] or thin layers of polydopamine adhesive [22]. However, chemical methods always involve the risk of introducing an intermediate adhesion material that may compromise biocompatibility [23].

The second approach is physical in nature and involves increasing the mechanical anchoring of CP coatings via the creation of micronanostructured surfaces. Iodine solution [24] and nitric acid [14] have been used to fabricate nanostructures on Au surfaces, which significantly improve the stability of PEDOT coatings. Nevertheless, these methods are mainly applicable to gold electrodes, but not to other substrates such as platinum and platinum–iridium (Pt–Ir) alloys, which are widely used for clinical applications. Femtosecond laser structuring, an emerging surface modification technique, is capable of producing various micro-nanostructures on the surfaces of different materials [25–27] via rapid resolidification after ablation and redeposition of nanoparticles generated during ablation [28]. Recently, it has been used to directly write on the Pt–Ir materials to generate hierarchical surfaces with a superwicking property [29]. The rich micro-nanostructure generated on the Pt–Ir substrate may provide abundant anchoring sites for CP coatings. Moreover, the superwicking property may improve the coating of substrates following immersion in an aqueous CP solution. However, additional tests are required to explore the stability of CP coatings on femtosecond laser-fabricated hierarchical structures.

In this study, PEDOT:PSS coatings were fabricated by drop casting (DC) and electrodeposition (ED) and applied to Pt–Ir substrates that were either hierarchically structured (hPt–Ir) or smooth Pt–Ir (sPt–Ir). Next, cyclic voltammetry stress and accelerated aging tests were performed to investigate the effects of substrate structures on the adhesion and stability of CP coatings.

Materials and methods

Electrode fabrication

The fabrication of Pt–Ir electrodes followed a previously established protocol [29, 30]. Bare Pt–Ir alloy tubes with an outer diameter of 1.27 mm and a wall thickness of 100 μm (composed of 90% Pt and 10% Ir, Johnson Matthey, USA) were used. Hierarchical structures were then created on the Pt–Ir substrates using a femtosecond laser system with the following optimized parameters: repetition rate, 100 kHz; pulse energy, 10 μJ; scanning speed, 5 mm/s; scanning interval, 8 μm. The laser-treated Pt–Ir tube was subsequently cut to a length of 1.5 mm to form electrode contacts. These were then cleaned by ultrasonication in water for 30 s to remove surface debris. Importantly, the sPt–Ir contact was directly cut from an untreated Pt–Ir tube. The contacts were connected to a copper bar using conductive silver glue (Ausbond 3813, China) and then placed on a polyurethane tube (Lubrizol, USA) with an outer diameter of 1.3 mm. Silicone rubber (K705, Kafuter, China) was used to seal all joints. Prior to the addition of coatings, all electrodes were rinsed in isopropanol and deionized water and then dried. The resulting sPt–Ir and hPt–Ir platforms are shown in Figs. 1a–1d and Fig. S1 (Supplementary Information). In brief, the presence of the hierarchical structure greatly increased the electrochemical performance of the hPt–Ir electrodes (as illustrated in Figs. 1e and 1f).

Preparation of PEDOT:PSS coatings

PEDOT:PSS coatings were prepared by drop casting (Fig. 1g) and electrodeposition (Fig. 1h) on both hPt–Ir and sPt–Ir electrodes.

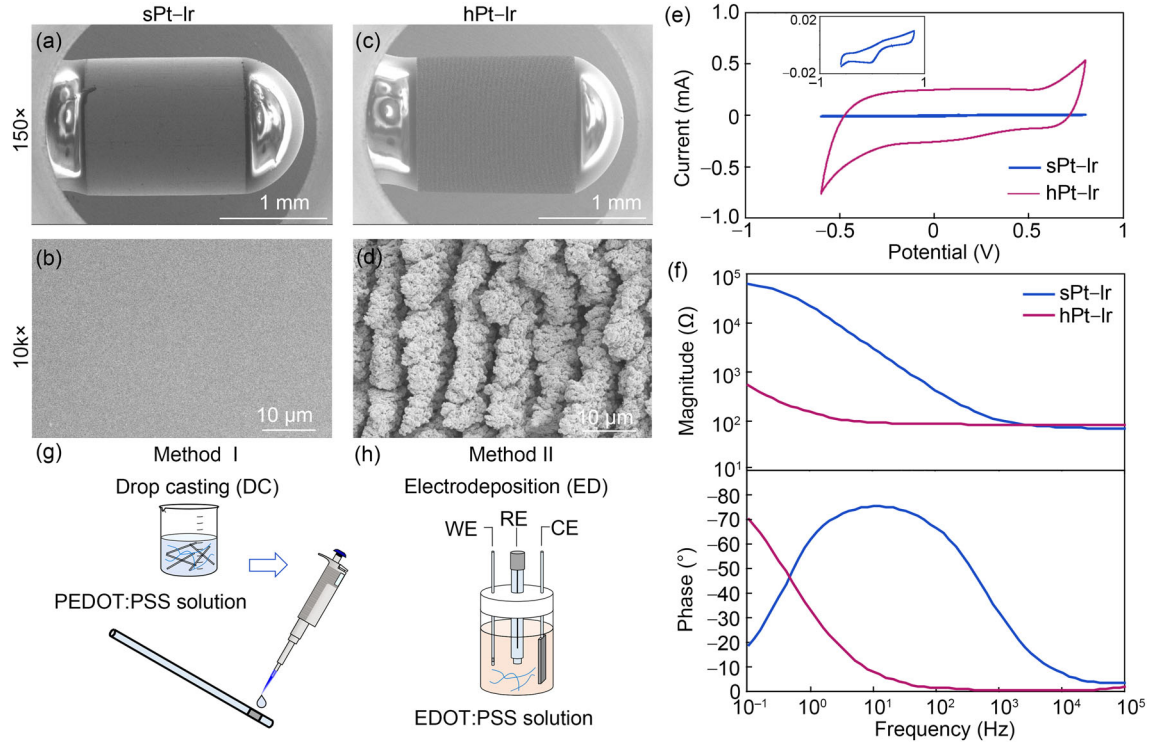

Fig. 1 Study overview. Microscopic morphology of smooth platinum–iridium (sPt–Ir) at magnifications of **a** 150× and **b** 10k× and hierarchical structures of platinum–iridium (hPt–Ir) at **c** 150× and **d** 10k×. **e** Cyclic voltammetry (CV) and **f** electrochemical impedance spectroscopy (EIS) performances of the sPt–Ir and hPt–Ir substrates. Two preparation methods of poly(3,4-ethylenedioxythiophene):poly(styrenesulfonate) (PEDOT:PSS) coatings including **g** drop casting and **h** electrodeposition. WE, RE, and CE represent the working electrode, reference electrode, and counter electrode, respectively

To prepare the drop cast PEDOT:PSS coating, the Pt–Ir contact was treated with air plasma for 2 min at a power of 100 W (Shanghai Zhongbin Technology, China). An aqueous dispersion of PEDOT:PSS (20 mL; Clavios PH 1000, Heraeus, Germany) was mixed with 5 mL of ethylene glycol, 50 μL of dodecylbenzene sulfonic acid, and 1% (mass fraction) of (3-glycidyloxypropyl)trimethoxysilane (Aladdin, China). Then, 1 μL of the solution was pipette-dropped onto sPt–Ir or hPt–Ir electrodes and cured at 45 °C for 4 h, 60 °C for 1 h, and for a final hour at 140 °C.

We used an electrochemical workstation (CHI 660E, CHI, China) with a three-electrode setup for the electrodeposition of the PEDOT:PSS coating. An sPt–Ir or hPt–Ir electrode was used as the working electrode, an Ag/AgCl electrode filled with a saturated KCl solution (Model 218, Leici, China) acted as the reference electrode, and a large titanium sheet (20 mm × 30 mm × 0.3 mm) was used as the counter electrode. PEDOT:PSS was then electrodeposited from 100 mmol/L EDOT (Aladdin, China) and 50 mmol/L sodium p-toluenesufonate (PSS, Aladdin, China) solutions in a solution containing a 1:1 ratio of acetonitrile and deionized water. Electrodeposition occurred under potentiostatic conditions at a potential of 1.4 V versus Ag/AgCl for 60 s.

Electrochemical performance testing

Electrode electrochemical performance was evaluated using a CHI 660E electrochemical workstation with the three-electrode configuration described above. Cyclic voltammetry (CV) and electrochemical impedance spectroscopy (EIS) were performed in 0.01 mol/L phosphate buffered saline (PBS) solution (P1000, Solarbio, China). This solution was prepared by dissolving one PBS tablet in 100 mL of deionized Milli-Q (Human Power I Plus, Republic of Korea) water. CV scans were then initiated using the open-circuit potential under voltages ranging from −0.6 to 0.8 V versus the reference electrode at a scanning rate of 50 mV/s. The charge storage capacity was determined by integrating the cathodic current density over time. For EIS testing, a 10 mV root-mean-square sinusoidal signal with zero direct current bias was applied, and the frequency sweep ranged from 0.1 Hz to 100 kHz.

Surface morphology characterization

The surface morphology of the PEDOT:PSS coatings was characterized using a high-resolution scanning electron

microscope (SEM, Helios G4 CX, FEI, USA) at a working voltage of 5 kV. To better characterize the cross-sectional structures of the coatings and substrates, focused ion beam (FIB) slicing was performed using the same equipment. Cross-sectional morphology was observed at a tilt angle of 40°.

Electrochemical stress testing

Cyclic voltammetry stress testing was performed within potential windows of −0.6–0.8 V relative to the Ag/AgCl electrode at a constant scanning rate of 100 mV/s in 0.01 mol/L PBS solution; this setup is depicted in Fig. S2a (Supplementary Information). The CV and EIS performances of the electrodes were characterized as previously described at different time points during the test, i.e., after 0, 250, 500, 1000, and 2000 CV cycles. Inspection by optical microscopy was also performed at the beginning and end of testing to assess the morphology of the coating. Finally, to gain further insight into the morphology of the coating, SEM and FIB slicing protocols were performed following stress testing.

Accelerated aging testing

Three electrodes of each type were used with different substrates for accelerated aging testing. As shown in Fig. S2b (Supplementary Information), electrodes were stored in PBS at 60 °C for five weeks and retrieved at 1-week intervals to perform EIS measurements and optical microscopic inspection (MV3000, Jiangnan Yongxin, China). For each combination of coating and substrate, the EIS values of the three samples were measured, and the impedance magnitude averages and their standard deviations at 1 kHz were then calculated. After aging testing, the coating morphology was observed using SEM.

Results

CV stress stability of DC coatings

The morphology and electrochemical performance of the DC coatings after CV stress testing are shown in Fig. 2. Inspection by optical microscopy revealed that after 2000 CV cycles, the DC coating of the sPt–Ir separated from the substrate and formed an arch shape (Figs. 2a and 2b). Further analysis using SEM revealed that the coating had bulged and delaminated from the substrate (Figs. 2c–2e). Electrochemical testing results showed that the area enclosed by the CV curve gradually decreased with increasing cycles, indicating a decrease in charge storage capacity (CSC) values (Fig. 2f). Meanwhile, the impedance magnitude gradually increased and the phase curve shifted to higher frequencies. This indicated degradation in the electrochemical behavior of the coating (Fig. 2g). Taken together, these results suggest that the PEDOT:PSS coating on the sPt–Ir electrode was unstable and experienced delamination and electrochemical performance deterioration during CV stress testing.

In contrast, the optical surface morphology of the DC coating on the hPt–Ir electrode remained stable after 2000 CV cycles (Figs. 2h and 2i). SEM image analysis at a magnification of 500× showed that the coating was uniform and free from damage (Fig. 2j). At higher magnifications (e.g., 10k× and 50k×, Figs. 2k and 2l), we found that the drop cast coating was well integrated into the micro-nanostructure of the substrate. This formed a highly enhanced mechanical anchor with a hierarchical structure. From an electrochemical perspective, the CV and EIS curves showed little change with increasing CV cycle (Figs. 2m and 2n). Stable morphology and electrochemical performance may be due to mechanical anchoring provided by the hierarchical structure present on the Pt–Ir surface, which acts to prevent deformation and maintain the integrity of the coating during cycling.

CV stress stability of ED coatings

Figure 3 shows the morphology and electrochemical performance of ED coatings following CV stress testing. We found that the ED coating of the sPt–Ir electrode experienced significant damage and electrochemical performance degradation after 2000 CV cycles. Analyses using optical microscopy and SEM revealed that over repeated cycles, the coating delaminated from the substrate around the cracks (Figs. 3a–3e). Thus, the area enclosed by the CV curve gradually decreased as the number of stress cycles increased, indicating a decreased CSC value (Fig. 3f). Similarly, the magnitudes of impedance also gradually increased, and the phase curve shifted to higher frequencies (Fig. 3g).

On the other hand, the ED coating of the hPt–Ir electrode exhibited stable morphology and electrochemical performance over 2000 CV cycles. The coating was uniform and showed no obvious damage. Moreover, it was present not only on the surface but also in the internal micro- and nanostructures beneath the surface. This is significant because it provides many anchor sites between the ED coating and the hierarchical structure (Figs. 3h–3l). Finally, changes in CV and EIS performance were quite small with increasing CV cycle number (Figs. 3m and 3n). Taken together, these results suggest that the enhanced interfacial adhesion provided by the hierarchical structure contributes to the stability of the morphology and electrochemical performance of the ED coating when present on the hPt–Ir electrode.

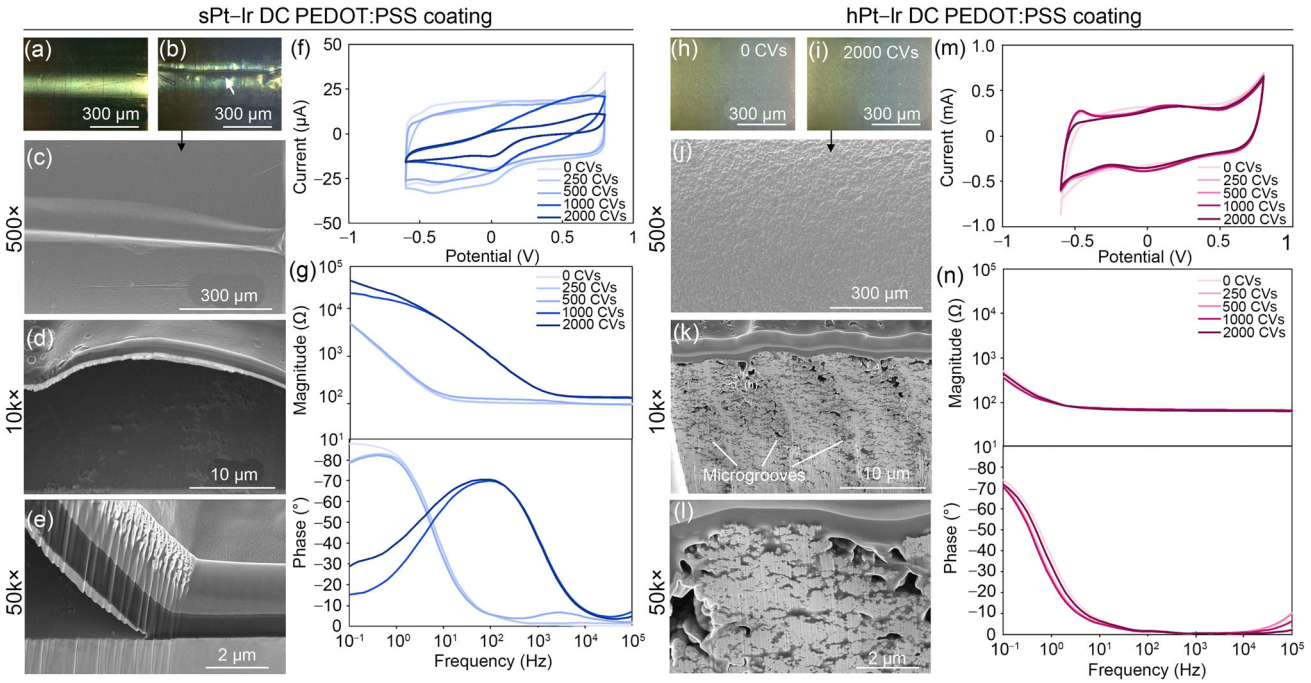

Fig. 2 Cyclic voltammetry (CV) stress testing results of drop cast coatings. Optical morphology of poly(3,4-ethylenedioxythiophene):poly(styrenesulfonate) (PEDOT:PSS) on sPt–Ir electrodes **a** before and **b** after 2000 CV cycles. Scanning electron microscope (SEM) morphology of the coating on sPt–Ir after 2000 CV cycles at magnifications of **c** 500×, **d** 10k×, and **e** 50k×. **f** CV curves and **g** electrochemical impedance spectroscopy (EIS) of the coating during 2000 CV cycles. Optical morphology of PEDOT:PSS on hPt–Ir electrodes **h** before and **i** after 2000 CV cycles. SEM morphology of the coating on hPt–Ir after 2000 CV cycles at **j** 500×, **k** 10k×, and **l** 50k×. **m** CV curves and **n** EIS of the coating during 2000 CV cycles. DC: drop casting

Accelerated aging stability

Figure 4 shows the results of the accelerated aging trials for the PEDOT:PSS coatings. The average change in impedance magnitude at 1 kHz frequencies in response to aging is shown in Fig. 4a. Results for other frequencies and complete scatterplots including all data points are shown in Figs. S3 and S4 (Supplementary Information), respectively. These results show that the sPt–Ir substrate, regardless of whether the PEDOT:PSS coating was added by DC or ED, exhibited a higher impedance increase than the hPt–Ir substrate. In addition, we observed that the DC coatings experienced a more pronounced rise in impedance than the ED coatings. Moreover, if the magnitude of the electrode impedance increased by more than 50% at 1 kHz, we designated it was nonfunctional. After five weeks of accelerated aging, we found that all of the DC and ED coatings on the sPt–Ir substrates were nonfunctional, whereas on the hPt–Ir substrate, all ED coatings and 67% of the DC coatings remained functional at the same time point (Fig. 4b, Fig. S5 in Supplementary Information). The surface morphologies of the DC and ED coatings on the sPt–Ir substrates showed delamination and cracking (Figs. 4c and 4e), respectively, whereas coatings added to the hPt–Ir substrate were relatively stable, with only one sample of cracking among the DC coating samples (Figs. 4d and 4f; Fig. S5 in Supplementary Information). Taken together, these results suggest that the hierarchical structures of the platinum–iridium substrate significantly improved the stability in performance of both coatings after aging.

Discussion

The use of conducting polymers as neural interface coatings has attracted attention because of their excellent electrochemical properties, high level of biocompatibility, and ease of fabrication. However, the long-term stability of these coatings is crucial for their use as neural probes in clinical applications. In this study, we prepared hierarchical structures on platinum–iridium substrates using femtosecond laser direct writing, and then investigated the effect of such structures on the stability of CP coatings when exposed to electrochemical stress and accelerated aging conditions.

Repeated scanning by cyclic voltammetry is often used as an accelerated testing protocol to evaluate the adhesion of conducting polymer films [14, 16, 21, 31, 32]. During scanning, ions are released or withdrawn from the electrolyte

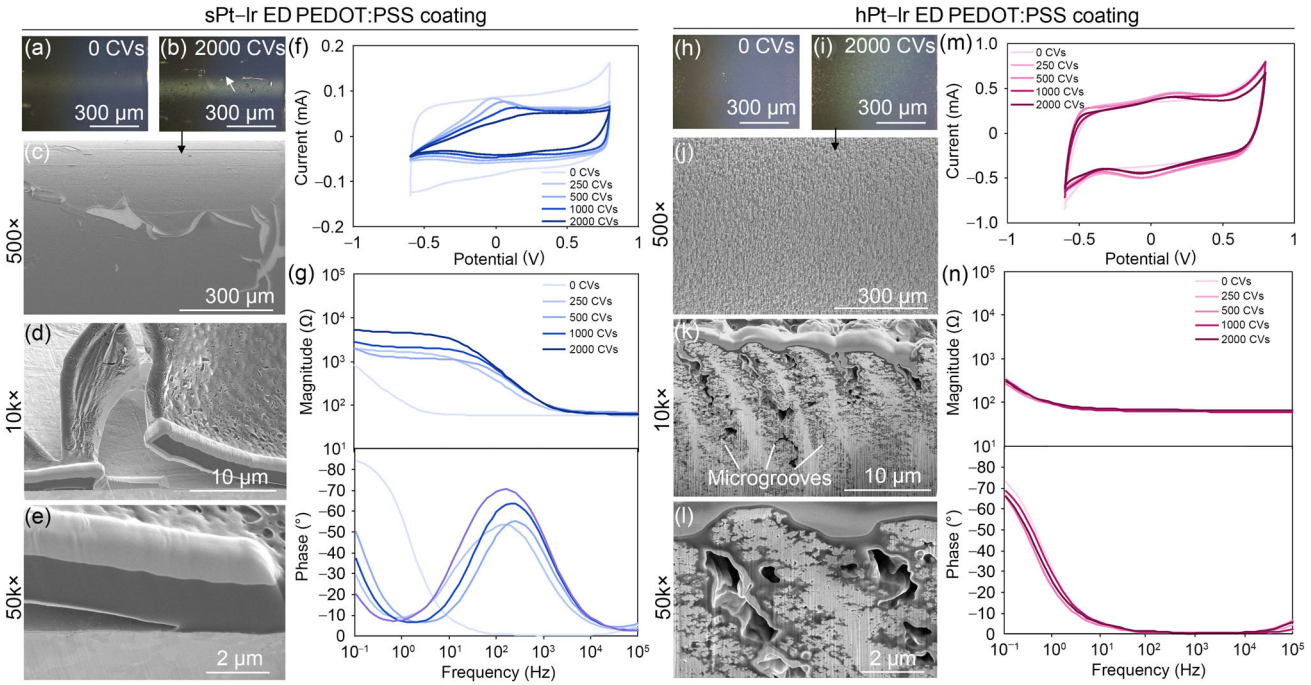

Fig. 3 Cyclic voltammetry (CV) stress testing results of electrodeposited coatings. Optical morphology of poly(3,4-ethylenedioxythiophene):poly(styrenesulfonate) (PEDOT:PSS) on sPt–Ir electrodes **a** before and **b** after 2000 CV cycles. Scanning electron microscope (SEM) morphology of the coating on sPt–Ir after 2000 CV cycles at magnifications of **c** 500×, **d** 10k×, and **e** 50k×. **f** CV curves and **g** electrochemical impedance spectroscopy (EIS) of the coating during 2000 CV cycles. Optical morphology of PEDOT:PSS on hPt–Ir electrodes **h** before and **i** after 2000 CV cycles. SEM morphology of the coating on hPt–Ir after 2000 CV cycles at **j** 500×, **k** 10k×, and **l** 50k×. **m** CV curves and **n** EIS of the coating during 2000 CV cycles. ED: electrodeposition

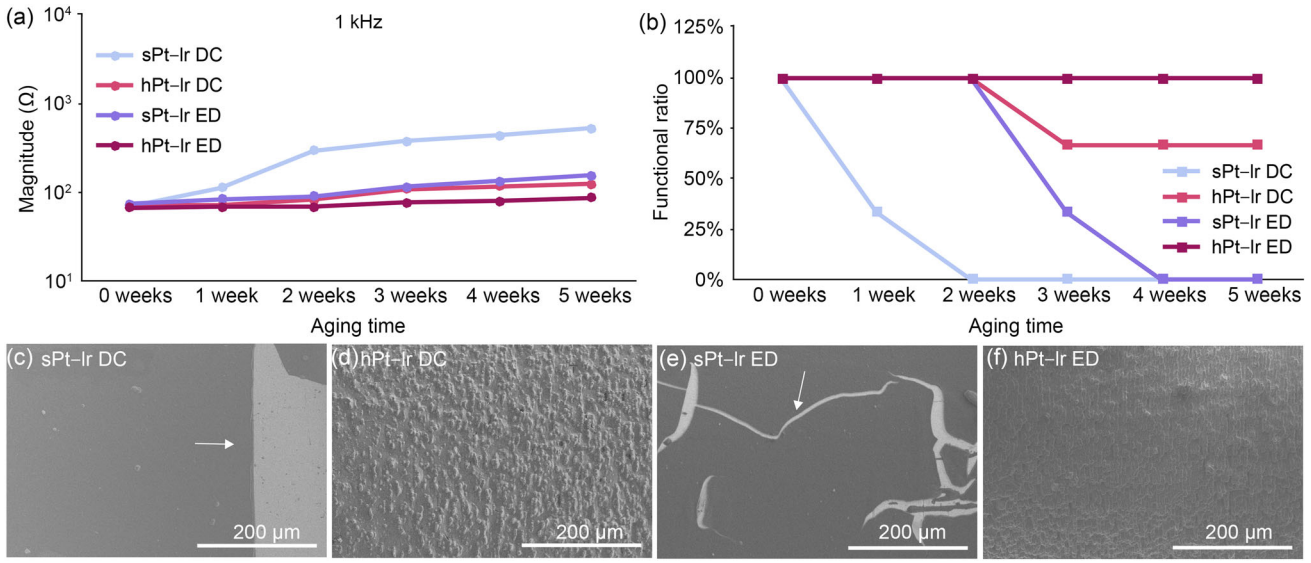

Fig. 4 Accelerated aging testing results of drop cast and electrodeposited poly(3,4-ethylenedioxythiophene):poly(styrenesulfonate) (PEDOT:PSS) coatings on sPt–Ir and hPt–Ir electrodes. **a** Average impedance magnitude at 1 kHz and **b** functional ratio of electrodes with aging time (a complete scatterplot including all data points is shown in Fig. S4 in Supplementary Information). Typical surface morphology of drop cast PEDOT:PSS on **c** sPt–Ir and **d** hPt–Ir electrodes and electrodeposited PEDOT:PSS on **e** sPt–Ir and **f** hPt–Ir electrodes after five weeks of accelerated aging. DC: drop casting; ED: electrodeposition

into the polymer bulk while reduction and oxidation reactions occur. The repeated shrinkage or expansion of the coating and chemical reactions that occur under applied potentials pose challenges to the adhesion of the CP coating on the substrate [31]. It is worth noting that biphasic current pulses commonly used in neurostimulation therapies generally do not involve high levels of stress. However, there are some notable exceptions to this principle, including applications such as the use of CV cycling to expel drugs from drug-loaded CP membranes [12].

In this study, the hierarchical structures present on platinum–iridium substrates were found to significantly improve the stability of both DC and ED coatings when exposed to repeated CV cycles; it is hypothesized that this occurs via enhanced mechanical anchoring. Previous studies have shown that PEDOT coatings on nanostructured platinum grass exhibit significantly increased impedance after hundreds of CV cycles [31]. However, hierarchical structures on platinum–iridium prepared using femtosecond laser direct writing have many available anchoring sites for the CP coating, especially beneath the surface (Figs. 2k and 3k). A recent study [29] explored the effect of femtosecond laser parameters on the surface morphology of Pt–Ir substrates. The prepared hierarchical structures generated microlumps at a period of 8 μm, which corresponded to the femtosecond laser scanning interval (Fig. S1d in Supplementary Information). Moreover, nanoparticles were generated with sizes ranging from tens to hundreds of nanometers (Fig. S1f in Supplementary Information). Among the microlumps, we observed microgrooves with depths greater than 10 μm (Fig. S1e in Supplementary Information; Figs. 2k and 3k). According to the CV results shown in Fig. 1e, the charge storage capacity of the femtosecond laser-prepared hPt–Ir electrode was 29.7 times greater than that of the smooth electrode. This increase in charge storage capacity indicates the greater surface area of the hPt–Ir substrate, which provides abundant mechanical anchor points for the coating. Enhanced mechanical anchoring can in turn help to resist electrochemical stress during the CV process, resulting in improved stability of PEDOT:PSS after 2000 cycles. Nevertheless, considering the complex interactions between hierarchical structures and CP coatings, surface area may not be the only factor affecting coating stability. Adjusting the femtosecond laser processing parameters can alter the pattern of micro- and nanostructures present on the surface [33, 34]. The effect of surface structures on the stability of coatings deserves further investigation in future work to decouple potential factors [18].

After CV stress testing, the presence or absence of different types of damage was determined for the DC and ED coatings on the smooth platinum substrates. Unlike the DC coating (Fig. 2c), the ED coating showed cracking in addition to delamination (Fig. 3c). These differences in damage may be attributed to film properties that differ due to differences in the two methods of coating fabrication. Compared with the direct molding of drop cast coatings, electrodeposited coatings gradually polymerize and thicken over time. Thus, as the thickness increases, the ED coating tends to crack [35, 36]. Accordingly, the initial defects of ED coatings may become more obvious as the coating delaminates following multiple CV cycles. Interestingly, ED coatings on substrates with hierarchical morphologies tended to avoid cracking during deposition and CV-induced stress (Fig. 3j). Recently, Mousavi et al. [35] found that coating cracking was related to the size and material properties of the substrate. However, the impact of different substrate structures on coating growth kinetics should be explored further in future studies.

In addition to active CV stress testing, passive testing in a humid environment was performed to rule out the effects of electrochemical stress [31]. A temperature of 60 °C is generally recommended for accelerated aging testing [14, 31, 37] because higher temperatures are believed to potentially cause internal decomposition of the polymer [38]. According to Arrhenius' law, the acceleration factor compared to body temperature (37 °C) is approximately 4.92; therefore, 5-week-long experiments simulated chronic implantation for a period of approximately six months.

As observed in CV stress testing, we found that the DC and ED coatings on the sPt–Ir substrate surface tended to delaminate and crack (respectively) after five weeks of aging. In contrast, on the hPt–Ir substrate, the stability of these two coatings was significantly improved. Nevertheless, one of the DC coatings on hPt–Ir tended to crack (Fig. S5 in Supplementary Information), whereas the ED coatings were more stable and exhibited a smaller rise in impedance than the DC coatings (Fig. 4). These findings are consistent with the results reported for Au nanorod substrates [14]. The low stability of conducting polymers may lead to biotoxicity within the bodies of implant recipients [39]. Doping carbon nanotubes in PEDOT has been proposed as a way to enhance coating stability, thereby facilitating neural recording and stimulation [40–42]. The impact of the composition and preparation process on the stability of conducting polymers deserves further investigation [39, 43–47].

Commonly used cyclic voltammetry and aging testing characterize coating performance to some extent, but quantitative characterization of the interfacial force may provide a direct evaluation of coating adhesion. Because of the small size of the electrode (i.e., approximately 1 mm in length) and the fragility of the thin coating around 1 μm, such measurements may be difficult to obtain. Nevertheless, quantitative assessment of interfacial force may provide a direct way to evaluate the adhesion mechanisms of hierarchical structures, which requires future exploration.

The in vivo stability and biocompatibility of CP coatings are also crucial for their use in clinical applications [23].

PEDOT:PSS coatings on substrates with hierarchical structures have exhibited significantly improved stability in vitro. This method shows good potential for neural stimulation in practical applications, especially for electrodeposited coatings. Furthermore, recent studies have validated the biosafety of conductive polymer coatings [14, 48] and hierarchical structures using Pt–Ir substrates [30]. However, the morphology of coatings on hierarchical structures can change, which may affect protein adhesion and cell and tissue growth [48, 49]. The in vivo environment contains various inorganic salts, proteins, and reactive oxygen species that may affect coating stability [50]. In addition, active tests, such as the application of biphasic pulse stimulation, can simulate the working conditions of clinical applications. Therefore, implantation experiments under neural stimulation may be useful for verifying the safety and efficacy of novel coatings for future applications [23, 50].

Femtosecond lasers with ultrashort pulses and ultrahigh power are not only suitable for micromachining of metallic materials but can also be used with soft materials such as polydimethylsiloxane (PDMS) [51] and polyimide (PI) [52]. Thus, they have attracted wide attention in the emerging field of soft bioelectrodes. Direct writing on the surfaces of soft materials with a femtosecond laser can not only directly pattern the conductive material, as has been demonstrated for laser-induced graphene [52], but can also adjust the roughness and wettability of surfaces [51]. Thus, these lasers are promising tools for the preparation of advanced bioelectrodes, and further investigation into their optimization should be an important research priority in the future.

Conclusions

PEDOT:PSS coatings on platinum–iridium substrates with hierarchical structures were found to exhibit highly stable electrochemical performance and morphology after 2000 cycles of CV stress tests or an aging test equivalent to half a year of implantation. In contrast, PEDOT:PSS coatings on smooth platinum–iridium substrates showed signs of damage and reduced electrochemical performance under the same conditions. We hypothesize that the improved mechanical anchoring provided by the hierarchical morphology of the platinum–iridium substrate can enhance the adhesion of the CP coating. These stable coatings may provide a crucial tool for the development of multimodal neural electrodes.

Supplementary Information The online version contains supplementary material available at https://doi.org/10.1007/s42242-024-00296-0.

Acknowledgements This work was supported by the National Key Research and Development Program of China (No. 2021YFC2400201), the National Natural Science Foundation of China (No. 81830033), the Natural Science Foundation of Fujian Province, China (No. 2023J05097), and the Young and Middle-aged Teacher Education Research Project of the Education Department of Fujian Province, China (No. JAT220004).

Author contributions Conceptualization, all authors; Methodology, LZL and CQJ; Investigation, LZL; Writing—original draft, LZL; Writing—review & editing, LZL and CQJ; Funding acquisition, all authors; Supervision, CQJ and LML.

Data availability Not applicable.

Code availability Not applicable.

Declarations

Conflict of interest LML is an editorial board member for *Bio-Design and Manufacturing*, and was not involved in the editorial review or the decision to publish this article. The authors declare that they have no conflict of interest.

Ethical approval This study does not contain any studies with human or animal subjects performed by any of the authors.

References

1. Cogan SF (2008) Neural stimulation and recording electrodes. Annu Rev Biomed Eng 10(1):275–309. https://doi.org/10.1146/annurev.bioeng.10.061807.160518
2. Zeng Q, Huang ZL (2023) Challenges and opportunities of implantable neural interfaces: from material, electrochemical and biological perspectives. Adv Funct Mater 33(32):2301223. https://doi.org/10.1002/adfm.202301223
3. Boehler C, Aqrawe Z, Asplund M (2019) Applications of PEDOT in bioelectronic medicine. Bioelectron Med 2(2):89–99. https://doi.org/10.2217/bem-2019-0014
4. Liang YY, Offenhäusser A, Ingebrandt S et al (2021) PEDOT:PSS-based bioelectronic devices for recording and modulation of electrophysiological and biochemical cell signals. Adv Healthc Mater 10(11):2100061. https://doi.org/10.1002/adhm.202100061
5. Lakard S, Pavel IA, Lakard B (2021) Electrochemical biosensing of dopamine neurotransmitter: a review. Biosensors 11(6):179. https://doi.org/10.3390/bios11060179
6. Mirza KB, Golden CT, Nikolic K et al (2019) Closed-loop implantable therapeutic neuromodulation systems based on neurochemical monitoring. Front Neurosci 13:808. https://doi.org/10.3389/fnins.2019.00808
7. Jones MG, Rogers ER, Harris JP et al (2021) Neuromodulation using ultra low frequency current waveform reversibly blocks axonal conduction and chronic pain. Sci Transl Med 13(608):g9890. https://doi.org/10.1126/scitranslmed.abg9890
8. Leal J, Shaner S, Matter L et al (2023) Guide to leveraging conducting polymers and hydrogels for direct current stimulation. Adv Mater Interface 10(8):2202041. https://doi.org/10.1002/admi.202202041
9. Leal J, Jedrusik N, Shaner S et al (2021) SIROF stabilized PEDOT/PSS allows biocompatible and reversible direct current stimulation capable of driving electrotaxis in cells. Biomaterials 275:120949. https://doi.org/10.1016/j.biomaterials.2021.120949
10. Aplin FP, Fridman GY (2019) Implantable direct current neural modulation: theory, feasibility, and efficacy. Front Neurosci 13:379. https://doi.org/10.3389/fnins.2019.00379

11. Merrill DR, Bikson M, Jefferys JGR (2005) Electrical stimulation of excitable tissue: design of efficacious and safe protocols. J Neurosci Method 141(2):171–198. https://doi.org/10.1016/j.jneumeth.2004.10.020
12. Boehler C, Oberueber F, Asplund M (2019) Tuning drug delivery from conducting polymer films for accurately controlled release of charged molecules. J Contr Release 304:173–180. https://doi.org/10.1016/j.jconrel.2019.05.017
13. Rudd S, Evans D (2022) Recent advances in the aqueous applications of PEDOT. Nanoscale Adv 4(3):733–741. https://doi.org/10.1039/d1na00748c
14. Ganji M, Hossain L, Tanaka A et al (2018) Monolithic and scalable Au nanorod substrates improve PEDOT-metal adhesion and stability in neural electrodes. Adv Healthc Mater 7(22):e1800923. https://doi.org/10.1002/adhm.201800923
15. Rossetti N, Hagler JE, Kateb P et al (2021) Neural and electromyography PEDOT electrodes for invasive stimulation and recording. J Mater Chem C 9(23):7243–7263. https://doi.org/10.1039/d1tc00625h
16. Ouyang LQ, Wei B, Kuo C et al (2017) Enhanced PEDOT adhesion on solid substrates with electrografted P(EDOT-NH_2). Sci Adv 3(3):e1600448. https://doi.org/10.1126/sciadv.1600448
17. Dalrymple AN, Robles UA, Huynh M et al (2020) Electrochemical and biological performance of chronically stimulated conductive hydrogel electrodes. J Neur Eng 17(2):26018. https://doi.org/10.1088/1741-2552/ab7cfc
18. Yang H, He T, Yan XX (2022) Adhesion strategies for heterogeneous soft materials—a review. Eng Res Express 4(1):12001. https://doi.org/10.1088/2631-8695/ac342e
19. Wei B, Liu JL, Ouyang LQ et al (2015) Significant enhancement of PEDOT thin film adhesion to inorganic solid substrates with EDOT-acid. ACS Appl Mater Interface 7(28):15388–15394. https://doi.org/10.1021/acsami.5b03350
20. Inoue A, Yuk H, Lu BY et al (2020) Strong adhesion of wet conducting polymers on diverse substrates. Sci Adv 6(12):eaay5394. https://doi.org/10.1126/sciadv.aay5394
21. Yang M, Yang TT, Deng HJ et al (2021) Poly(5-nitroindole) thin film as conductive and adhesive interfacial layer for robust neural interface. Adv Funct Mater 31(49):2105857. https://doi.org/10.1002/adfm.202105857
22. Tian FJ, Yu JW, Wang W et al (2023) Design of adhesive conducting PEDOT-MeOH:PSS/PDA neural interface via electropolymerization for ultrasmall implantable neural microelectrodes. J Colloid Interface Sci 638:339–348. https://doi.org/10.1016/j.jcis.2023.01.146
23. Shepherd RK, Villalobos J, Burns O et al (2018) The development of neural stimulators: a review of preclinical safety and efficacy studies. J Neur Eng 15(4):41004. https://doi.org/10.1088/1741-2552/aac43c
24. Pranti AS, Schander A, Bödecker A et al (2018) PEDOT:PSS coating on gold microelectrodes with excellent stability and high charge injection capacity for chronic neural interfaces. Sens Actuat B Chem 275:382–393. https://doi.org/10.1016/j.snb.2018.08.007
25. Zhang KD, Deng JX, Guo XH et al (2018) Study on the adhesion and tribological behavior of PVD TiAlN coatings with a multi-scale textured substrate surface. Int J Refract Hard Met 72:292–305. https://doi.org/10.1016/j.ijrmhm.2018.01.003
26. Park J, Park B, Son YJ et al (2021) Femtosecond laser-mediated anchoring of polymer layers on the surface of a biodegradable metal. J Magnes Alloy 9(4):1373–1381. https://doi.org/10.1016/j.jma.2020.12.003
27. Zhang PJ, Zou XR, Zhang SL et al (2021) Improve the binding force of PEEK coating with Mg surface by femtosecond lasers induced micro/nanostructures. J Mater Sci 56(23):13313–13322. https://doi.org/10.1007/s10853-021-06140-5
28. Vorobyev AY, Guo CL (2013) Direct femtosecond laser surface nano/microstructuring and its applications. Laser Photonics Rev 7(3):385–407. https://doi.org/10.1002/lpor.201200017
29. Li LZ, Jiang CQ, Li LM (2022) Hierarchical platinum-iridium neural electrodes structured by femtosecond laser for superwicking interface and superior charge storage capacity. Bio-Des Manuf 5(1):163–173. https://doi.org/10.1007/s42242-021-00160-5
30. Li LZ, Jiang CQ, Duan WR et al (2022) Electrochemical and biological performance of hierarchical platinum-iridium electrodes structured by a femtosecond laser. Microsyst Nanoeng 8(1):96. https://doi.org/10.1038/s41378-022-00433-8
31. Boehler C, Oberueber F, Schlabach S et al (2017) Long-term stable adhesion for conducting polymers in biomedical applications: IrOx and nanostructured platinum solve the chronic challenge. ACS Appl Mater Interface 9(1):189–197. https://doi.org/10.1021/acsami.6b13468
32. Ji BW, Wang MH (2020) Micro-wrinkle strategy for stable soft neural interface with optimized electroplated PEDOT:PSS. J Micromech Microeng 30(10):104001. https://doi.org/10.1088/1361-6439/aba5db
33. Chen ZJ, Yang J, Liu HB et al (2022) A short review on functionalized metallic surfaces by ultrafast laser micromachining. Int J Adv Manuf Technol 119(11–12):6919–6948. https://doi.org/10.1007/s00170-021-08560-8
34. Förster DJ, Jäggi B, Michalowski A et al (2021) Review on experimental and theoretical investigations of ultra-short pulsed laser ablation of metals with burst pulses. Mater 14(12):3331. https://doi.org/10.3390/ma14123331
35. Mousavi H, Ferrari LM, Whiteley A et al (2023) Kinetics and physicochemical characteristics of electrodeposited PEDOT:PSS thin film growth. Adv Electron Mater 9(9):2201282. https://doi.org/10.1002/aelm.202201282
36. Niederhoffer T, Vanhoestenberghe A, Lancashire HT (2023) Methods of poly(3,4)-ethylenedioxithiophene (PEDOT) electrodeposition on metal electrodes for neural stimulation and recording. J Neur Eng 20(1):11002. https://doi.org/10.1088/1741-2552/acb084
37. Wang XY, Yang HR, Zhang BH et al (2023) The integrated rGO/PEDOT:PSS-modified ultraflexible microelectrodes towards long-term neurophysiological signaling and dopamine sensitive detection. In: Proceedings of the IEEE 36th International Conference on Micro Electro Mechanical Systems (MEMS), p.297–300. https://doi.org/10.1109/MEMS49605.2023.10052189
38. Boehler C, Carli S, Fadiga L et al (2020) Tutorial: guidelines for standardized performance tests for electrodes intended for neural interfaces and bioelectronics. Nat Protoc 15(11):3557–3578. https://doi.org/10.1038/s41596-020-0389-2
39. Zhang M, Gao B, Liu JD et al (2022) The stability of poly(3,4-ethylenedioxythiophene) based on electrochemical polymerization and photoelectro-corrosion conditions. Polym Degrad Stabil 198:109881. https://doi.org/10.1016/j.polymdegradstab.2022.109881
40. Zheng XS, Yang QR, Vazquez A et al (2022) Imaging the stability of chronic electrical microstimulation using electrodes coated with PEDOT/CNT and iridium oxide. iScience 25(7):104539. https://doi.org/10.1016/j.isci.2022.104539
41. Kozai TDY, Catt K, Du ZH et al (2016) Chronic in vivo evaluation of PEDOT/CNT for stable neural recordings. IEEE Trans Biomed Eng 63(1):111–119. https://doi.org/10.1109/TBME.2015.2445713
42. Gerwig R, Fuchsberger K, Schroeppel B et al (2012) PEDOT–CNT composite microelectrodes for recording and electrostimulation applications: fabrication, morphology, and electrical properties. Front Neuroeng 5:8. https://doi.org/10.3389/fneng.2012.00008
43. Schultheiss A, Gueye M, Carella A et al (2020) Insight into the degradation mechanisms of highly conductive poly(3,4-ethylenedioxythiophene) thin films. ACS Appl Polym Mater 2(7):2686–2695. https://doi.org/10.1021/acsapm.0c00301

44. Oldroyd P, Malliaras GG (2022) Achieving long-term stability of thin-film electrodes for neurostimulation. Acta Biomater 139:65–81. https://doi.org/10.1016/j.actbio.2021.05.004
45. Sordini L, Garrudo FFF, Rodrigues CAV et al (2021) Effect of electrical stimulation conditions on neural stem cells differentiation on cross-linked PEDOT:PSS films. Front Bioeng Biotechnol 9:591838. https://doi.org/10.3389/fbioe.2021.591838
46. Cellot G, Lagonegro P, Tarabella G et al (2016) PEDOT:PSS interfaces support the development of neuronal synaptic networks with reduced neuroglia response in vitro. Front Neurosci 9:521. https://doi.org/10.3389/fnins.2015.00521
47. del Agua I, Mantione D, Ismailov U et al (2018) DVS-crosslinked PEDOT:PSS free-standing and textile electrodes toward wearable health monitoring. Adv Mater Technol 3(10):1700322. https://doi.org/10.1002/admt.201700322
48. Zhang ZY, Tian GZ, Duan XG et al (2021) Nanostructured PEDOT coatings for electrode-neuron integration. ACS Appl Bio Mater 4(7):5556–5565. https://doi.org/10.1021/acsabm.1c00375
49. Woeppel KM, Cui XT (2021) Nanoparticle and biomolecule surface modification synergistically increases neural electrode recording yield and minimizes inflammatory host response. Adv Healthc Mater 10(16):2002150. https://doi.org/10.1002/adhm.202002150
50. Dijk G, Rutz AL, Malliaras GG (2020) Stability of PEDOT:PSS-coated gold electrodes in cell culture conditions. Adv Mater Technol 5(3):1900662. https://doi.org/10.1002/admt.201900662
51. Liang C, Su WM, Sun XY et al (2021) Femtosecond laser patterning wettability-assisted PDMS for fabrication of flexible silver nanowires electrodes. Adv Mater Interface 8(19):2100608. https://doi.org/10.1002/admi.202100608
52. Wagh MD, Renuka H, Kumar PS et al (2022) Integrated microfluidic device with MXene enhanced laser-induced graphene bioelectrode for sensitive and selective electroanalytical detection of dopamine. IEEE Sens J 22(14):14620–14627. https://doi.org/10.1109/JSEN.2022.3182293